Contents lists available at ScienceDirect

Microchemical Journal

journal homepage: http://ees.elsevier.com

Optical reflectance apparatus for moisture content determination in porous media

J. Melada, P. Arosio, M. Gargano, I. Veronese, S. Gallo, N. Ludwig *

Dipartimento di Fisica, Università degli Studi di Milano, Via Celoria 16, 20133 Milano, Italy

A B S T R A C T

Monitoring surface moisture content (*MC*)is a required activity and a topic of current interest in conservation studies. The present work examines the possibility of using the spectral reflectance factor at 970 nm ($R_\lambda 970$) for the noninvasive quantitative determination of surface *MC* in building materials. Indeed, the quantification of surface liquid water by optical measurements is poorly exploited on porous media despite it is well documented in many remote sensing technologies such as in agriculture, soil science and some industrial application. The measurements apparatus is tested in a laboratory experiment on different specimens of building materials. The custom-made detector is a Si-core Avalanche Photo Diode (APD) operating in Geiger mode which satisfy the requirements of non-invasiveness and ease of use with the additional opportunity for developing economic, automated and reliable solutions. The results obtained for six representative cultural heritage building materials clearly show the dependence between $R_\lambda 970$ and surface *SMC*: $R_\lambda 970$ increases as surface *MC* decrease following the drying process of an unsaturated porous matrix i.e. evaporative flux supported by capillary pumping. This work reports the possibility to use the reflectance value at a specific wavelength for an alternative and non-invasive measurements of MC.Keywords NIR spectroscopy; water absorption; moisture content; building materials.

1. Introduction

The deterioration and degradation of materials surface in historic construction is often linked to the presence of water [1]. Indeed, many forms of decay are related to the content of water inside a material, e.g. freeze-thaw cycles and salts crystallization cycles. For this reason, the accurate assessment of moisture content (*MC*) of porous materials is needed. Most of the deterioration processes involve the transport of gases, liquids and ions and the moisture level plays a crucial role in all these processes and their comprehension is of the utmost importance in any methodology of moisture content measurement [2]. This study examines the possibility of using a characteristic absorption band of liquid water in the near infrared at 970 nm ($R_\lambda 970$) for a quantitative determination of the surface moisture content (*MC*) in porous media. The definition of a standard procedure for the determination of surface *MC* in historical materials is currently an open challenge in conservation studies [3]. Non-invasive and non-destructive measurements are preferable in cultural heritage applications due to the high relevance of the objects. To extend the measurements on the largest number of objects, the methodology should also ideally be cheap, easy to perform, reproducible and non-invasive. In addition, it would be desirable that the measure methodology is able to quantitatively and continuously measure *MC*. Indeed, the establishment of thermohygrometric cycles or abrupt changes in *MC* must be monitored, since they are extremely harmful for the materials conservation. It is also necessary to understand the advantages and disadvantages of this specific methodology since it provides a superficial information i.e. surface moisture content. Actually, the moisture distribution along the thickness of a wall is spatially heterogeneous [4]. The study of the external layers of the material is however crucial in evaluating the decay processes due to water transport phenomena in between material microstructure and environment [5]. If the increase of moisture is detected before the visible effects occur, then early conservation procedures can be started. It must be remarked that the quantitative determination of *MC* in common porous geomaterials is strictly connected with the determination of the material's porosity and water pathways [6]. Indeed, the study of porosity, and hygric properties of building materials is a fundamental step for evaluating their state of conservation and planning correct restoration projects [7].

2. Moisture content measurements in cultural heritage

The visualization of the spatial and temporal distribution of *MC* is very useful to test and predict the time dependant behaviour and degradation processes of weathered structures and the performance of materials used for restoration [6]. The methods currently used to determine *MC* can be divided in two categories: destructive methods

* Corresponding author.
E-mail address: nicola.ludwig@unimi.it (N. Ludwig)

https://doi.org/10.1016/j.microc.2020.104627
Received 30 August 2019; Received in revised form 13 December 2019; Accepted 8 January 2020
Available online xxx
0026-265/

and non-destructive methods. Destructive methods require the sampling of the material while non-destructive methods do not require intervention in the structure of the object. Moisture content (*MC*) is the quantity of moisture inside a material as a result of exchange between the material and the surrounding environment [8]. It is classically gravimetrically defined as the percentage ratio between the mass of water (m_w) inside a material and the mass of the dry material (m_d) itself:

$$MC = \frac{m_w}{m_d} \cdot 100$$

The moisture content of a material is determined by its hygroscopicity and varies with the microenvironmental conditions. Recently a new standard for the determination of moisture content specifically intended for the application on cultural heritage has been developed. The standard EN 16682 – Conservation of Cultural Heritage – Methods of measurements of moisture content, or water content, in materials constituting immovable cultural heritage establishes priorities between methods [3]. Despite the existence of this standard, there are only few studies in the literature that exploit the optical reflectance measure of *MC* on porous materials with reference to building materials and cultural heritage. The most popular methodologies for the measurement of *MC* have been well described in [1,3,8–10].

2.1. Optical reflectance for the determination of moisture content

Optical remote sensing is an interesting methodology to measure surface *MC* at high spatial and temporal resolution since water in the outer pores causes a change in scattering and absorption of light [11]. Usually reflectance measurements assume that the reflectance of a moist material decrease in the near infrared as the *MC* increase [12]. It is expected that measuring the spectral reflectance factor in specific bands it is possible to estimate the material's surface *MC* [13]. Some authors have observed the change in spectral reflectance of porous media such as soil or building materials and they have found empirical predictive relationship between surface *MC* and R_λ that however are generally influenced by the nature of the solid material itself [14,15]. Pure liquid water in NIR shows five predominant absorption bands at 760 nm, 970 nm, 1190 nm, 1450 nm, 1940 nm [16]. The present study considers the 970 nm absorption band that is attributed to a combination of symmetric and asymmetric stretching of the molecules ($a\nu_1 + b\nu_3$, where $a + b = 3$) [17]. Indeed, one of the main advantages of working in this region of the spectrum is the possibility of using a Silicon solid state detector, that is cheaper than other detectors working in longer wavelength ranges. The determination of relative reflectance values implies that for each type of material a dry reference spectrum is available, so each further surface *MC* estimation based on the relative reflectance approach relies on the existence and the accuracy of the reference reflectance spectrum [12]. However, if the surface changes over time, the optical properties of that dry surface could be affected, leading to drift in measurements [9]. In this context, the possibility of using a reference material of the same type to obtain reference curves without sampling should be evaluated. A high spectral reflectance factor difference between saturated and dry state is needed for the distinction of intermediate moisture levels. Otherwise, it would require very accurate radiometric calibration, also considering other parameters affecting surface reflectance (e.g. mineral composition, pore size distribution, surface roughness, coatings and above all different colours) that may vary under field conditions [11]. Usually a normalized absorption band depth is utilized as reference since this approach is independent to the materials characteristics and only affected by the presence of water. However, this approach cannot be used at 970 nm since the optical path length in common geomaterials is short with respect to the attenuation length of water at this wavelength [14]. Optical sensing has both advantages and disadvantages: this methodology is able to identify the moist areas independently to the surface temperature in a non-invasive way, on the other hand radiation in the visible and near infrared does not penetrate materials beyond the surface layer, generally consisting of some microns [14]. This limited penetration is balanced by the ability to take observations at high spatial resolution over large areas.

3. Materials and methods

3.1. Specimens

Cultural heritage materials are very heterogeneous. Six different type of representative building materials with a wide range of hygroscopic parameters have been considered: stone, brick and two plasters furthermore we tried to study the behaviour of wooden materials such as hardwood and softwood. Ten specimens for each type of material were prepared. The specimens were cylinders with a known and defined geometry and similar dimensions. Stones and bricks samples (MB and LT) were obtained with a 2.7 cm external diameter hole saw obtaining a final diameter of 2.5 cm. Mortars (MA) and plasters (IC) samples were prepared in wooden moulds of 2.5 cm diameter.

Wood specimens (PS and SM) are taken from planks of solid wood with a 3.0 cm external diameter hole saw with a final diameter of 2.7 cm. PS is made of pine wood and SM is made of Mahogany wood.

The mean values of volume (*V*), density (ρ_{dry}), imbibition capacity *(CI)* and open porosity *(WIP)* for the 10 specimens and for each material are reported in Table 1. The water imbibition capacity (*CI*) is defined by the standard UNI Normal-7/81 [18]. *WIP* is determined using the saturation or immersion technique which determines the open porosity of a material by saturating a specimen with a liquid of known density and calculating the pore volume from the weight difference between the fully saturated and dry state as described in [19]. As can be noted, marble (MB) has the higher ρ_{dry} and the lower *CI* and *WIP*. Wood specimens presents the higher imbibition capacity and lower dry density: Brick (LT), mortar (MA) and plaster (IC) have similar values of dry density and imbibition capacity. In Fig. 1 it is possible to observe the dependence of the porosity (*WIP*) to the dry density of the materi-

Table 1
Sample mean and standard deviation of volume, dry density, imbibition capacity and open porosity of each type of material.

Specimens	*V* (cm ^{3})	ρ_{dry} (g/cm ^{3})	*CI* (%)	*WIP* (%)
MB	7.72 ± 0.07	2.65 ± 0.02	0.52 ± 0.13	1.58 ± 0.50
LT	7.94 ± 0.14	1.85 ± 0.02	16.63 ± 0.11	30.92 ± 0.36
PS	10.01 ± 0.23	0.57 ± 0.02	131.64 ± 4.50	75.25 ± 2.10
SM	9.86 ± 0.31	0.62 ± 0.02	86.69 ± 2.61	53.67 ± 1.84
MA	11.31 ± 0.76	1.63 ± 0.06	19.68 ± 0.62	29.52 ± 1.32
IC	10.43 ± 0.60	1.48 ± 0.04	20.67 ± 0.38	30.12 ± 0.92

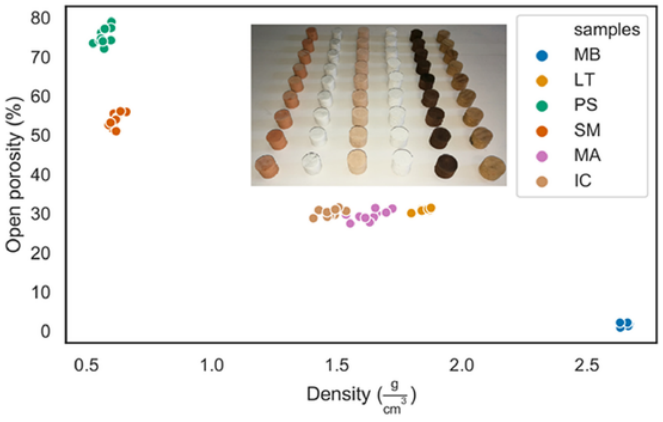

Fig. 1. Relationship between open porosity (WIP) and dry density. increasing the dry density, the WIP decreases'.

als. Because of swelling of wood specimens due to water imbibition we used for *WIP* determination the volume in saturation condition.

Surface *MC* was measured with the help of a non-invasive reflectance measurement device. The optical detector was a custom-made photon counting system based on a silicon APD (C309021S, Perkin Elmer Optoelectronics, Canada) operating in Geiger mode already developed in [20,21]. The APD was characterized by a quantum efficiency (QE) curve extending beyond 1000 nm. The package of the detector chip contained a light-pipe (core diameter 0.25 mm, numerical aperture 0.55) which fell within the active area of the detector, allowing efficient coupling with the optical fibre. During operation, the APD was cooled down to a temperature of approximately −19 °C by means of a two-stage Peltier thermoelectric cooling system. The operating temperature was monitored by a K-type thermocouple (Analog Devices Inc., MA, USA) positioned in the detector chip support. A specific circuit was implemented to quench and digitalize the APD breakdown pulse. A data-acquisition device (DAQ USB-6000, National Instruments, TX, USA) was used to acquire the count rate, together with the thermocouple output. A specific program was implemented in the LabView environment (National Instruments) to process and analyse the signals. An optical fibre conveys the light from the light source to the specimen and another one takes the reflected light from the specimen to the detector. A band-pass filter with centre peak wavelength at 970 nm (Thorlabs GmbH) and FWHM of 10 nm is placed at the entrance of the detector. This is necessary for measuring the reflectance only in the water characteristic absorption band at 970 nm.

3.2. fibre-holder and light source

To ensure repeatable measurement conditions a fibre-holder in black polylactide (PLA) have been designed and 3D-printed. The fibre-holder has three holes for the accommodation of the optical fibres at −45°, 0°, 45° with respect to the normal. The base has a 6 cm diameter hole that forms a cylindrical black box allowing to host the specimen and to perform the measurements without saturate and damage the highly sensitive photodetector. The light spot area on the specimen is about 7 cm^2. The light was brought to the specimen with an optical fibre at 45° with respect to the normal. A 0° fibre optics conveyed the reflected light to the detector through the 970 nm bandpass filter. The measurement geometry was 45°x:0° The specimen during the measurements was housed in a hole of the base with a diameter of 3 cm and a depth of 2 cm to ensure to measure only the whole specimen's surface. The light source was an incandescent bulb HL-2000-FHSA and the reference ideal diffusor was a Spectralon® white standard (Labsphere).

3.3. Spectral reflectance factor measurements

The spectral reflectance factor (R_λ) is the ratio of the reflected radiant flux in a given solid angle centred at the centre of the sampling aperture on the surface of the specimen and the one reflected in the same direction by an equally illuminated ideal reflective diffuser. The percentage spectral reflectance factor (R_λ) is calculated as follows:

$$R_\lambda = \frac{C_x - C_{\text{black}}}{C_{\text{standard}} - C_{\text{black}}} \cdot 100$$

Where C_x are the photons counted by the detector at different *MC,* C_{black} are the dark counts and C_{standard} are the counts on the reflectance standard. The reflectance measurements were performed on all the sixty specimens described in Section 4. Specimens were monitored from fully saturated to dry state twice a day for 5 days by gravimetry (paragraph 3.2.4) and optical reflectance measurements. Saturation occurred by total immersion in deionised water until the constant mass have been reached. Each specimen was then covered with Parafilm M leaving only one face free to ensure evaporation and transport of water only in one direction. The drying of the specimens was carried out in a climatic chamber at $t = 25$ °C and $RH = 50\%$ with moderate ventilation of about 5 m/s. Each measure is the average of 30 s of data acquisition for the following drying steps: 12 h, 24 h, 36 h, 48 h, 60 h, 72 h, 84 h, 96 h. To avoid errors in the measurements due to an instrumental drift and to have comparable data between the various specimens the C_{black} and C_{standard} were measured before and after each counting acquisition. The complete dry-state measures were acquired after oven-drying the specimens for one night at 102 °C. The surface *MC* of the specimens in the results section is presented in relation to their saturation state (*SG*), i.e. $SG = 100\%$ for saturated specimens and $SG = 0\%$ for dry specimens. This is defined as:

$$SG = \frac{m_x - m_d}{m_{sat} - m_d} \cdot 100$$

where m_x is the mass of the wet specimen at each measure condition, m_d is the dry mass of the specimen and m_{sat} is the saturated mass of the specimen.

4. Results and discussion

4.1. Laboratory test on geomaterials specimens

The reflectance measurements were performed on all the forty specimens. Fig. 2a, b, c and –d shows the measured R_λ as a function of *SG* of each specimen. Presenting the data, it was decided to not add the error bars to increase data readability since the mean absolute error for each data point is < 3% having the same dimensions of the graphic point. Decreasing *SG* a non-linear increase of R_λ is observed over the full drying process for marble (MB), brick (LT), plaster (IC) and mortar (MA).

In this kind of situation, i.e. one directional transport of moisture, there is an approximately linear dependence of the spectral reflectance factor to the moisture content only in a finite range of high moisture content. After a threshold value of *MC* (identify in this study as SG_{tv}), R_λ became almost constant and do not contain any additional information about the moisture content of the material. Below SG_{tv} water front should be held tightly inside the materials matrix as adsorbed water films around the walls of pores and capillaries. Consequently, the evaporation occurs inside the specimens. Here the optical path length in water is null, and the measured value of the spectral reflectance factor is almost solely due to material's surface absorption and scattering. Otherwise at high levels of *SG*, water fills surface layers increasing the optical path length in water which led to decreasing the values of R_λ. The actual value of SG_{tv} has not been reported in this study due to the acquisition rate; as showed in Fig. 2 even the trend is evident, the gap between the data point doesn't allow us to define SG_{tv} with enough precision. Indicatively for MB, MA and IC a plateau is reached at about 50 and 60 units. In addition, brick specimens (LT) presents also two stages in the variation of R_λ: an approximately constant value for $80\% < SG < 100\%$ and a sharp variation for $SG = 80\%$ and $SG = 45\%$. As previously said, the determination of *MC* based on a single-band reflectance values implies the availability and representativeness of a dry reference reflectance standard. Fig. 3 highlight this problem: the spectral reflectance factor of each material's specimen is not constant in the dry and saturated state. Indeed, the distribution of values. The same is for the saturated state. Moreover, for mahogany specimens (*SM*) $R_{\lambda,sat} > R_{\lambda,dry}$. This means that each specimen needs a specific reference curve. In other words, the curves are strongly dependant on the specific specimen and not for the overall material. This could be explained by the local variability of the surface's colour and roughness. In a hypothetical in-situ application it could be of difficult application because it is not always possible to have at disposal the dry reference material. Moreover, the possibility to perform measurements at high spatial resolution, which is one of the main demands of this methodology, could not be applicable on materials with heterogeneous surface properties. The drying process of the specimens was observed thanks to the drying curves. Examples are shown in Fig. 2e and f where

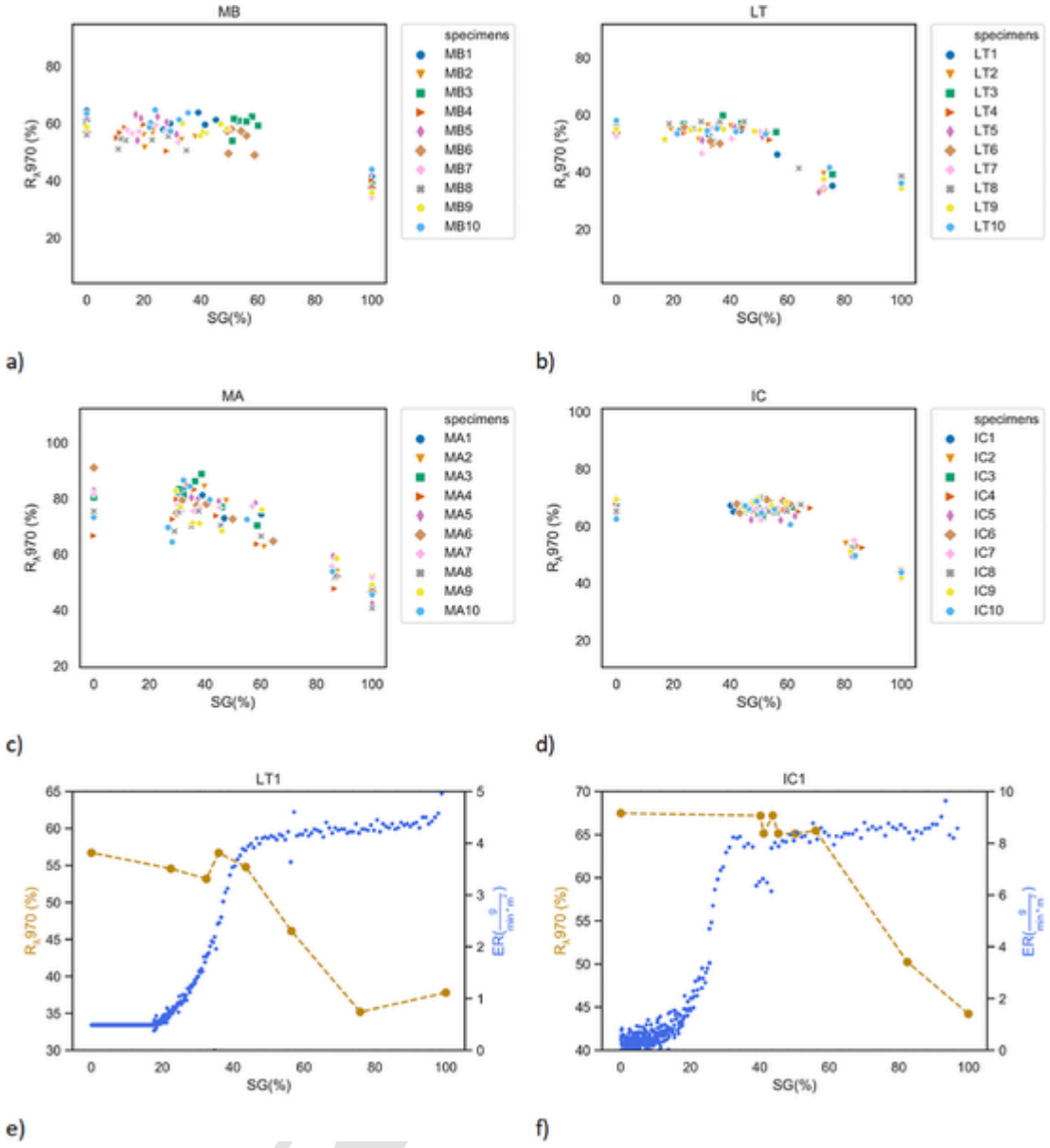

Fig. 2. Variation of measured spectral reflectance factor at 970 nm ($R_\lambda 970$) at different values of saturation grade (SG) for a) marble specimens, b) brick specimens, c) putty-lime plaster specimens, d) plaster with cocciopesto specimens. And variation of measured spectral reflectance factor at 970 nm ($R_\lambda 970$) at different values of saturation grade (SG) for e) brick specimen LT1 and f) plaster specimen IC1.

the curves show the variation of the evaporation rate or evaporative flux (*ER*) in function of the *MC*. It was not reliable to measure *ER* of MB1 due to electronic balance readings fluctuations caused by the ventilation rate and of course due to its intrinsic low value of *CI*.

When the breakthrough point is reached the liquid-gas interface cannot recede any further from the open pores close to the surface and the front position becomes almost constant over a wide range of *MC*. The constant rate period is usually longer in larger pore networks. As *MC* decreases the larger pores are drained and will no longer contribute to liquid transport [22]. This result confirms that spectral reflectance is influenced by surface moisture content and it is linked to the hydraulic behaviour of water in the unsaturated matrix. Although it is beyond the scope of the present work, it would be interesting to verify if this value can be linked both to the water front depth or to the critical moisture content. It will be necessary to repeat these experiments on the same material with different thicknesses and geometries. Furthermore, the impact of degradation products and restoration products on the modality of moisture diffusion in porous materials must be evaluated.

4.2. Laboratory test on wood specimens

Wood specimens R_λ dependence of *SG* is more complicated. The increase of spectral reflectance upon drying is non-linear. As it is possible to observe in Fig. 4a and b the spectral reflectance factor of the wood specimens does not depend by *MC* like the other specimens. A possible explanation of this phenomenon could be the peculiar way in which wood exchanges moisture with the environment. Indeed, the drying process of wood is driven mainly by water bounded to the sorption sites below the fibre saturation point and by free water above it [23]. Another hypothesis could invoke the structural anisotropies of wood, i.e. the directions of the fibers and grains, which can affect the spatial distribution of the reflected radiation. Initially, this problem had not been considered since, as previously mentioned in Section 2.2, the spectral reflectance factor can be considered as averaged on a circular area of about 7 cm^2. However, the laws of radiation's diffusion

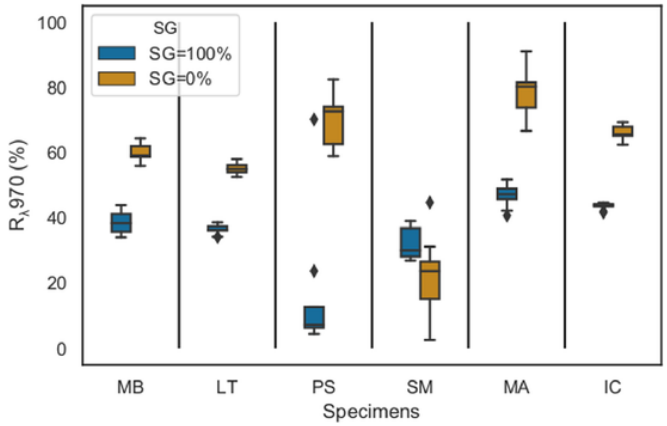

Fig. 3. Paired boxplot of the spectral reflectance factor at 970 nm ($R_\lambda 970$) of the ten specimens of each material in saturated (SG = 100%) and dry conditions (SG = 0%).

vary with the dimensions of the optical non-homogeneities of the medium. A further test has been arranged to verify whether the direction of the fibers influences the measured signal with respect to the acquisition geometry. The test was performed with two wooden specimens (PS1 and SM1) and one brick specimen for comparison (LT1). The measurement took place both on specimens in saturated by total immersion condition and overnight oven-dried condition. The measurement took place by marking a reference point on the cylindrical specimens and acquiring the value of $R_{\lambda,sat}$ and $R_{\lambda,dry}$ by rotating the specimen on a reference plane of about 90° at each measurement. Each acquisition was repeated 4 times; between each repetition at every angle the lid of the measuring chamber was opened to verify that the movement of the optical fibers did not influence the data. The bar-plots in Fig. 4c, d and e show that the spectral reflectance factor varies as a function of the angle between the specimen and the direction of the incident light. The reference direction (0°) was taken randomly on the brick sample and marked on the side with an indelible marker. For wood, it was chosen along the direction of the wood's fibers. The spectral reflectance factor of the brick specimen remains constant while the specimen rotates with respect to the illumination direction. The spectral reflectance factor changes considerably for woods, even up to 10 percentage units, depending on the direction of illumination. The spectral reflection factor is therefore higher when the direction of the fibers is perpendicular to the direction of illumination.

5. Discussion

Such a measurement method could be improved in many ways by using different radiation (i.e. microwave) or other infrared bands [24]. In the past our group worked in the use of infrared thermography [25] that is able to evaluate the amount of evaporation rate in a totally noninvasive way. The use of a set of multiple reflectance values acquired in differed band of the (NIR) spectrum namely at about 1450 and 1930 nm, is well known but in the years, it never becomes an affordable method in moisture detection. The use of silicon-based detector, suitable for 970 nm absorption peak detection, instead of InGaAs one could help the diffusion of this kind of measurements. Another issue concerning the portability and repeatability of the instrumentation regards the selection of the light source which should follow these requirements: strong light emission in the water absorption bands of interest, low power consumption, avoid surface heating and avoid complicated and fragile optical components. An incandescent lamp, as the one used in this study, only meets some of the requirements. It is easy to use and relatively economic, but it could present some drawbacks in the in-situ application. Indeed, in this study, it has been mandatory to use a band-pass filter placed in front of the detector. As drawback, optical systems can complicate the development of instruments that are easily portable and usable in situ. Beside this the incandescent lamp would allow the multi band reflectance measurements. It could be interesting to study the applicability of Light Emitting Diodes (LED) with narrow emission spectrum which combine the low power consumption with a narrow band emission making unnecessary the use of band pass filters. Again, it must be reminded that this device allows to get only superficial information, and therefore has the disadvantages and the advantages already highlighted. Such a non-invasive and non-destructive methodology provides an opportunity to perform measurements in many measuring points allowing to obtain surface *MC* profiles

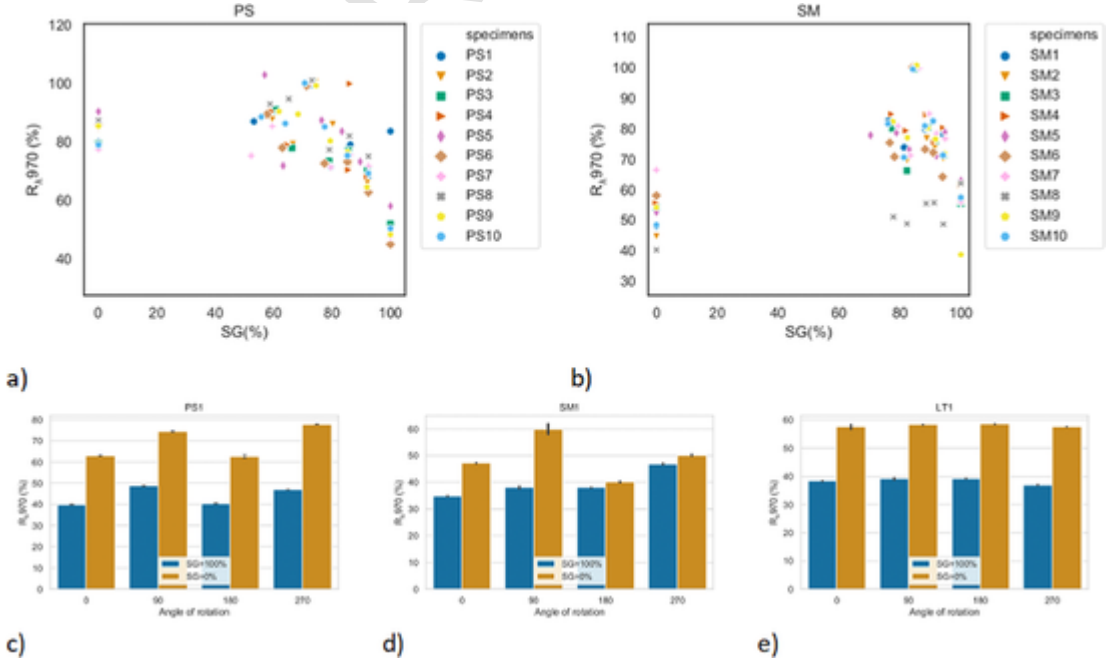

Fig. 4. Variation of measured spectral reflectance factor at 970 nm ($R_\lambda 970$) at different values of saturation grade (SG) for a) pine solidwood specimens, b) mahogany solidwood specimens. And variation of the spectral reflectance factor while rotating the specimen of c) pine solidwood, d) mahogany solidwood, e) brick specimens according to the direction of the incident light.

and maps. These profiles can be very useful to determine the causes of moisture in wall and to plan correct remediation interventions [4]. To measure water in depth it is certainly recommended to couple this sensor with other methods of investigation, for example microwave methods [15]. Therefore, it is again stressed out that it is mandatory to choose an appropriate method for the specific situation and accurately select the profile or the point in which perform the measurements [4].

6. Conclusions

The use of optical remote sensing in the measure of surface MC for the considered materials, showed to be more effective when measured in a finite range of moisture content values. Indeed, the increase of spectral reflectance upon drying follows the hydraulic behaviour of water in the unsaturated solid matrix. In laboratory conditions, data exhibited a threshold value of surface *MC*, specific of the type of material, at which the relation between R_λ and MC suddenly changes. Below this value R_λ varies approximately linearly with *MC* and above it R_λ% is quite constant. This was confirmed also by comparing the evaporation curves with the relationship between R_λ and *MC*. Indeed, this method, directly related to the superficial water content, can be easily compared with the steady method of passive thermography that indirectly measures the moisture content through the measurement of the evaporative flux. The use of the custom-made APD for the quantitative assessment of *MC* meets the requirements of non-invasiveness, simplicity, accuracy and the possibility of developing economic and automated solutions. Beside this, the measurement system could be optimized considering other variables involved in the mechanism of evaporation. We, in fact, simplified the problem of moisture transport considering a single direction of water, contrary to the direction of the gravity acceleration. It would be necessary to verify if these results shall be applicable on a real case, where in addition to the problem of three-dimensional moisture transport there is the presence of salts, restoration materials, fluctuations of environmental parameters, and spatial heterogeneity (both lateral and in thickness of the materials).

A further improvement could be aimed to study the variation of R_λ in multiple absorption bands since at 970 nm the light may not provide enough contrast in dry and saturated signal to differentiate intermediate moisture levels. Additionally, it will be useful to evaluate the possibility of compaction of the system to increase its portability and ease of use, firstly by choosing a lighting source that avoids the use of optical filters.

CRediT authorship contribution statement

J. Melada: Investigation, Writing - original draft, Visualization. **P. Arosio:** Validation. **M. Gargano:** Writing - review & editing, Data curation. **I. Veronese:** Conceptualization. **S. Gallo:** Writing - review & editing, Software. **N. Ludwig:** Supervision, Methodology, Writing - review & editing.

Declaration of Competing Interest

None.

References

[1] D Camuffo, Microclimate for Cultural Heritage: Conservation, Restoration, and Maintenance of Indoor and Outdoor Monuments, Elsevier Science, 2013.

[2] L-O Nilsson (Ed.), Methods of Measuring Moisture in Building Materials and Structures, Methods of Measuring Moisture in Building Materials and Structures, Springer International Publishing, Cham, 2018, doi:10.1007/978-3-319-74231-1.

[3] D Camuffo, Standardization activity in the evaluation of moisture content, J. Cult. Herit. 31 (2018) S10–S14, doi:10.1016/J.CULHER.2018.03.021.

[4] A Hola, Measuring of the moisture content in brick walls of historical buildings – the overview of methods, IOP Conf. Ser. Mater. Sci. Eng. 251 (2017), doi:10.1088/1757-899X/251/1/012067 012067.

[5] N Ludwig, E Rosina, A Sansonetti, Evaluation and monitoring of water diffusion into stone porous materials by means of innovative IR thermography techniques, Measurement 118 (2018) 348–353, doi:10.1016/J.MEASUREMENT.2017.09.002.

[6] Z Kis, F Sciarretta, L Szentmiklósi, Water uptake experiments of historic construction materials from Venice by neutron imaging and PGAI methods, Mater. Struct. 50 (2017) 159, doi:10.1617/s11527-017-1004-z.

[7] M Brai, C Casieri, F De Luca, P Fantazzini, M Gombia, C Terenzi, Validity of NMR pore-size analysis of cultural heritage ancient building materials containing magnetic impurities, Solid State Nucl. Magn. Reson. 32 (2007) 129–135, doi:10.1016/J.SSNMR.2007.10.005.

[8] D. Camuffo, C. Bertolin, e-Preservationscience towards standardisation of moisture content measurement in cultural heritage materials, n.d.www.e-PRESERVATIONScience.org (accessed August30, 2019).

[9] W.H.-A. transactions, undefined2003, Moisture sensor technology-a summary of techniques for measuring moisture levels in buildling envelopes, search.proquest.com.(n.d.). http://search.proquest.com/openview/e6748ed48927f79d1471dfac76507c0a/1?pq-origsite=gscholar&cbl=34619 (accessed August 30, 2019).

[10] I. Mundula, N. Tubi, Umidità e risanamento negli edifici in, muratura, (1997).

[11] C Nolet, A Poortinga, P Roosjen, H Bartholomeus, G Ruessink, Measuring and modeling the effect of surface moisture on the spectral reflectance of coastal beach sand, PLoS ONE 9 (2014), doi:10.1371/journal.pone.0112151 e112151.

[12] S -N. Haubrock, S Chabrillat, C Lemmnitz, H Kaufmann, Surface soil moisture quantification models from reflectance data under field conditions, Int. J. Remote Sens. 29 (2008) 3–29, doi:10.1080/01431160701294695.

[13] B G Heusinkveld, S M Berkowicz, A F G Jacobs, W Hillen, A A M Holtslag, A new remote optical wetness sensor and its applications, Agric. For. Meteorol. 148 (2008) 580–591, doi:10.1016/J.AGRFORMET.2007.11.007.

[14] J Tian, W D Philpot, Relationship between surface soil water content, evaporation rate, and water absorption band depths in SWIR reflectance spectra, Remote Sens. Environ. 169 (2015) 280–289, doi:10.1016/J.RSE.2015.08.007.

[15] D Magrini, C Cucci, R Olmi, M Picollo, C Riminesi, Investigation on water content in fresco mock-ups in the microwave and near-IR spectral regions, Meas. Sci. Technol. 28 (2017), doi:10.1088/1361-6501/aa533f 024003.

[16] J A Curcio, C C Petty, The near infrared absorption spectrum of liquid water, J. Opt. Soc. Am. 41 (1951) 302, doi:10.1364/JOSA.41.000302.

[17] A Iakovenko, V Iashin, A Kovalev, E F- Biofizika, undefined, Vibrational structure of absorption spectra of water in visible region, Europepmc.Org. (2002) (n.d.), https://europepmc.org/abstract/med/12500558 (accessed August 30, 2019).

[18] NorMaL, 7/81: assorbimento d'acqua per immersione totale–Capacità di imbibizione, CNR Centri Di Stud. Di Milano e Roma Sulle Cause Di Deperimento e Sui Metod. Di Conserv. Delle Opere d'arte–ICR Ist. Cent. per Restauro, Roma. (1981).

[19] U Kuila, D K McCarty, A Derkowski, T B Fischer, M Prasad, Total porosity measurement in gas shales by the water immersion porosimetry (WIP) method, Fuel 117 (2014) 1115–1129, doi:10.1016/J.FUEL.2013.09.073.

[20] J Melada, M Gargano, I Veronese, N Ludwig, Does electro-osmosis work in moisture damage prevention? Applicability of infrared-based methods to verify water distribution under electric fields, J. Cult. Herit. (2018) 31, doi:10.1016/j.culher.2018.04.009.

[21] I Veronese, N Chiodini, S Cialdi, E D'ippolito, M Fasoli, S Gallo, S La Torre, E Mones, A Vedda, G Loi, Institute of Physics and Engineering in Medicine 1361-6560/17/104218+19$33.00 © 2017 Institute of Physics and Engineering in Medicine Printed in the UK, Phys. Med. Biol. 62 (2017) 4218–4236, doi:10.1088/1361-6560/aa642f.

[22] C Nunes, L Pel, J Kunecký, Z Slížková, The influence of the pore structure on the moisture transport in lime plaster-brick systems as studied by NMR, Constr. Build. Mater. 142 (2017) 395–409, doi:10.1016/j.conbuildmat.2017.03.086.

[23] E T Engelund, L G Thygesen, S Svensson, C A S Hill, A critical discussion of the physics of wood-water interactions, Wood Sci. Technol. 47 (2013) 141–161, doi:10.1007/s00226-012-0514-7.

[24] P Bison, G Cadelano, L Capineri, D Capitani, U Casellato, P Faroldi, E Grinzato, N Ludwig, R Olmi, S Priori, N Proietti, E Rosina, R Ruggeri, A Sansonetti, L Soroldoni, M Valentini, Limits and advantages of different techniques for testing moisture content in masonry, Mater. Eval. 69 (2011) 111–116, https://www.researchgate.net/publication/286982060 (accessed December 10, 2019).

[25] E Grinzato, N Ludwig, G Cadelano, M Bertucci, M Gargano, P Bison, Infrared thermography for moisture detection: a laboratory study and in-situ test, Mater. Eval. 69 (2011) 97–104.